Available online at www.sciencedirect.com
ScienceDirect
Journal of Electrical Systems and Information Technology 5 (2018) 135–143
www.elsevier.com/locate/jesit

Control of fuzzy logic based PV-battery hybrid system for stand-alone DC applications

Neerparaj Rai [a,*], Bijay Rai [b]

[a] *Department of Electrical Engineering, Dr B.R. Ambedkar Institute of Technology, India*
[b] *Department of Electrical Engineering, Sikkim Manipal Institute of Technology, India*

Received 27 December 2016; received in revised form 5 August 2017; accepted 24 February 2018
Available online 27 March 2018

Abstract

The paper presents a hybrid system comprising of photovoltaic (PV) and battery with fuzzy logic control (FLC) to meet the demands of isolated off grid DC loads. Perturb and Observe (P&O) method is used to achieve the maximum power point tracking (MPPT) by controlling the duty cycle of a dc–dc boost converter. Fuzzy logic controller regulates the power flow of the battery by means of a bidirectional buck-boost converter. The complete energy management system has been validated in MATLAB/SIMUINK with variable solar irradiation profile. The simulation results show that the system with fuzzy logic control prolongs the battery lifespan by reducing the battery peak current up to 0.22% and also significantly decreases the settling time and peak overshoot of the DC load voltage up to 16.23% and 14.62% as compared to the system with conventional PID control.

Keywords: Photovoltaic; Fuzzy logic controller; Bidirectional converter

1. Introduction

Due to the fast depletion of fossil fuel and increasing pollution rate renewable energy sources have become most effective source of energy. But the major challenge in integration of these renewable sources is its intermittent nature and cost. PV is one of the most effective renew-able energy sources, but it is not available at night time. This ensures the requirement of two or more renewable energy sources (Torreglosa et al., 2014). Therefore, to make this kind of hybrid system more reliable and cost effective, there must be some energy storage devices to store the available energy when available and also feed the load under low PV output situations. Battery and Super Capacitor (SC) are used for storage purposes. The important advantage of battery over SC is its high energy density. They can store at least 3–30

* Corresponding author.
Peer review under the responsibility of Electronics Research Institute (ERI).

Production and hosting by Elsevier

https://doi.org/10.1016/j.jesit.2018.02.007

times more charge than SC (Thounthong et al., 2009). Whereas, SCs are able to deliver hundred to thousand time more power than a similar sized Battery (Weddell et al., 2011). So Battery is able to supply long term energy demand compared to SC.

Under all operating conditions, there is a point on the P–V curve at which entire PV system operates. This allows the operation to take place producing maximum output power with maximum efficiency. Many MPPT methods have been developed and implemented. The methods vary in complexity, sensors required, convergence speed, cost, implementation hardware, range of effectiveness, popularity, and in other respects (Faranda et al., 2008; Rohrig and Lange, 2008; Faranda and Leva, 2008; Salas et al., 2006; Esram and Chapman, 2007; Zegaoui et al., 2011). To incorporate MPPT tracking, an intermediate DC–DC boost converter is proposed which is controlled by Perturb & Observe (P&O) method. The MPP tracking is applied to a standalone PV system in order to extract maximum available power at all values of solar irradiation and temperature. The P&O technique (Femia et al., 2005; Femia et al., 2007), which is based on iterative algorithms are widely used since it is easy to implement with rapid tracking capabilities and minimum steady state oscillations.

Many researchers have focused their study on control of hybrid system. Garca et al. (2013) have studied FC-battery-SC based hybrid system to supply hybrid vehicles type load. Glavin et al. (2008) have studied control of PV-SC-Battery based hybrid energy system. Guiting et al. (2013) have implemented flatness based control strategy and classical PI controller based control to study PV-FC-SC energy system respectively. Thounthong et al. (2013) have taken PVFC Battery-SC based hybrid system for their study.

In this paper a fuzzy logic controller (FLC) for maintaining a constant DC link voltage for standalone PV applications is proposed. PV is used as the primary energy source but due to the fluctuating nature of the PV power supply, a battery is connected in parallel as a back-up energy storage system. Perturb and Observe control algorithm based MPPT controller gives the required duty cycle to achieve MPP. Bidirectional dc–dc buck-boost converter is used for controlling the power flow from the battery. A FLC controller was designed to regulate the duty ratio of the MOSFET switches to maintain power balance in the standalone system under varying solar irradiation conditions. The proposed hybrid system can be implemented in rural households for lightning purpose and running isolated pumps for effective harvesting.

The modelling of the complete hybrid system is carried out in Section 2 which includes modelling of solar PV module and designing of FLC and PID controller. In Section 3, the effects of irradiance change on the DC bus voltage, battery current and SOC of the battery is presented. MPPT tracking results for P&O controls are also included in Section 3. Finally the conclusion is presented in Section 4.

2. Modelling of hybrid system

The proposed hybrid energy system considering PV-Battery is shown in Fig. 1. The system is used to supply a standalone DC load at a constant voltage. In this paper, PV is used as the primary source while battery is used as the back-up energy storing element. A boost converter is used to interface the PV arrays with the load. MPPT based on P&O technique is implemented to always extract maximum available solar power. A FLC based control strategy for DC–DC bidirectional buck/boost converter is adopted to keep the DC link voltage constant during changes in solar irradiation. Charging and discharging of the battery is controlled depending on the DC bus voltage.

2.1. Modelling of PV module

A PV cell generates around 0.5 V–0.8 V depending upon the semiconductor material and the technology used. Due to the small value of the voltage it cannot be used as a single PV cell. Therefore, the PV cells are connected in series to increase the voltage (i.e. from 36 to 72 cells) to form a PV module. The set of PV cells are also connected in parallel to achieve higher value of output current.

This paper carried out a Matlab/Simulink model of 200 W, 12 V PV module for which four parallel sets of 36 cells are used. The developed model allows the prediction of the output which can be PV current, voltage or power. The weather data such as irradiance and temperature are considered as input variables. The model is based on mathematical equations and any change in the input variables causes an immediate change in the output parameter.

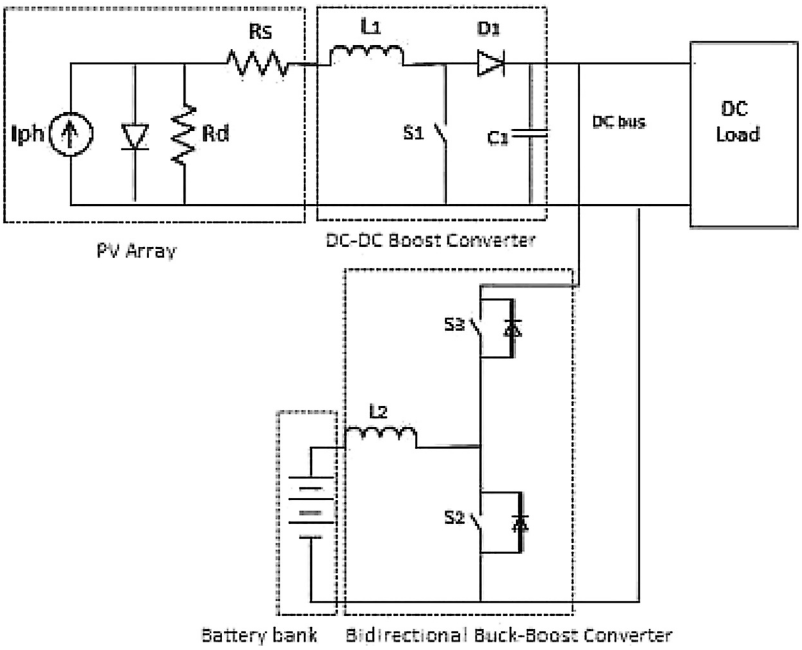

Fig. 1. Structure of PV-battery hybrid system.

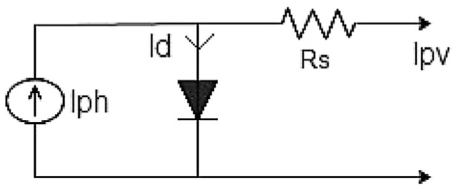

Fig. 2. The equivalent circuit of a PV cell.

The I–V characteristic of a PV cell is not linear and depends on multiple parameters. While modelling a PV cell, series resistance R_s and shunt resistance R_p of the cell are considered for precise and accurate results. The shunt resistance being very large, some authors neglects the incorporation of shunt resistance in the modelling of a PV cell. The focus of the paper is to design a simplified solar cell model to show the effectiveness of the solar charge controller under different situations. Therefore, an ideal PV cell is modelled using a current source in parallel with a diode and a series resistance R_s. Using Kirchhoff law, the current to the load I_{pv} can be written as:

$$I_{pv} = I_{ph} - I_d \tag{1}$$

In Eq. (1), I_{ph} is the photocurrent produced from the PV cell. The PV cell photocurrent depends on the solar radiation and the temperature according to Eq. (2).

$$I_{ph} = [I_{scr} + K_i (T - T_r)] \left(\frac{S}{1000} \right) \tag{2}$$

where S: Solar radiation (W/m^2), T_r: Cell temperature under standard test condition (STC) = 273 + 25 = 298 K, T: Actual cell temperature (Kelvin), K_i: Temperature coefficient of the cell's short circuit current (0.0023 A/K), I_{scr}: Reference photocurrent under standard test conditions (0.0023 A).

The diode current shown in Fig. 2 I_d is proportional to the reverse saturation current I_{rs} as given by the Eq. (3).

$$I_d = I_{rs} \left[\exp \left(\frac{V}{A N_s V_T} \right) - 1 \right] \tag{3}$$

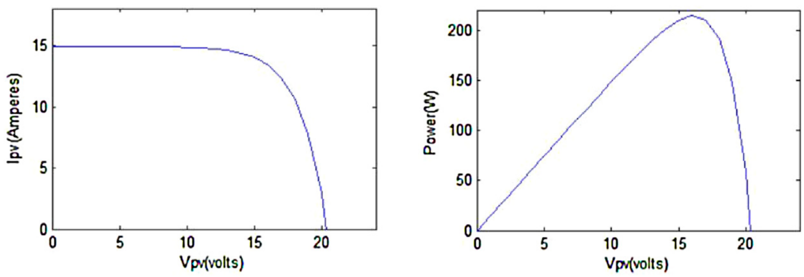

Fig. 3. (a) I–V curve of the PV model. (b) P–V curve of the PV model.

where, V is the voltage across the diode, A is the ideality factor of the diode, N_s is the number of PV cells in series ($N_s = 36$) and V_T is called the thermal voltage which is a function of temperature.

$$V_T = \frac{k.T}{q} \tag{4}$$

where, k is the Boltzmann's constant (1.381×10^{-23}) and q is electron charge (1.602×10^{-19} C). Recombining the above two Eqs. (3) and (4) we arrive to Eq. (5).

$$I_d = I_{rs}\left[\exp\left(\frac{qV}{k.T.A.N_s}\right) - 1\right] \tag{5}$$

The diode reverse saturation current is defined by Eq. (6).

$$I_{rs} = I_{rr}\left(\frac{T}{T_r}\right)^3 \exp\left[\left(\frac{q.E_q}{A.k}\right)\left(\frac{1}{T_r} - \frac{1}{T}\right)\right] \tag{6}$$

The diode reverse saturation current varies as a cubic function of the temperature. Eg is the band gap energy of the semiconductor (1.166 eV) and I_{rr} is the reference value of the reverse saturation current under STC (0.000021 A).

Finally, the PV array output current (I_{pv}) is obtained using the mathematical Eqs. (5) and (7). N_p is the number of PV cells is parallel ($N_p = 4$).

$$I_{pv} = N_p.I_{ph} - N_p.I_d \tag{7}$$

In this PV model, four parallel sets of 36 PV cells in series are interconnected to form one PV module of 200 W, 12 V rating. The I–V and P–V simulation of the designed PV module in Fig. 3(a) and (b) show that the open circuit voltage is nearly 21.5 V and the short circuit current is 11.3A for a solar radiation of 1000 W/m^2 and temperature of 298 K.

2.2. MPPT control (P&O)

Perturbation and observation method is also known as hill climbing method (Hill Climbing, HC). Its working principle is making a small active voltage perturbation in a certain working voltage of photovoltaic cells and observing the change direction of output power. If the output power increases then perturbation in the same direction should be kept, otherwise perturbation against the original direction should be made. Since the PV array is interfaced using a boost converter, the PV voltage is increased by decreasing the duty ratio of the converter and vice versa.

Fig. 4 summarizes the control action of the P&O method. If the PV voltage is perturbed in a particular direction and the product of change in power and voltage is positive ($\Delta P \times \Delta V > 0$), means the operating point is moving towards MPP. Therefore the duty ratio is further reduced to increase the PV voltage. Otherwise, if ($\Delta P \times \Delta V < 0$) then the operating point has moved away from MPP and the P&O algorithm reverses the direction of the perturbation by increasing the duty ratio of the boost converter.

In this paper, perturbation and observation method is applied to extract maximum power from PV which operates by sensing the PV voltage (V_{pv}) and PV current (I_{pv}). The MPPT controller always regulates PV power to its maximum power. If more power is available it will always go to charge the battery.

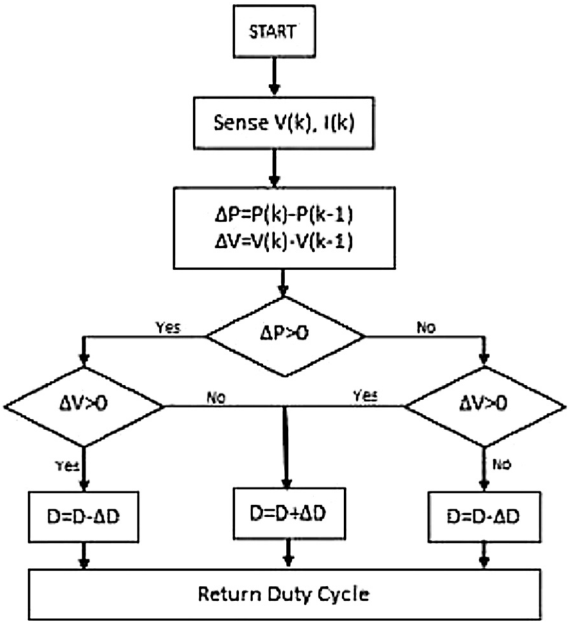

Fig. 4. The flowchart of the P&O MPPT method.

2.3. *Fuzzy logic controller*

The battery serves as the back-up and long term energy storage element in the proposed hybrid system. It helps to compensate for the fluctuating PV power output by storing the excess power and also discharging during low PV power situations. Battery bank is driven by two quadrant bidirectional dc–dc converter. The FLC controller changes the duty ratio for the switches S2 and S3 of the bidirectional converter to switch and regulate the mode of operation from charging to discharging. In the simulations, battery discharging current is considered to be positive whereas battery charging current as negative.

A fuzzy logic controller is designed to control the charging and discharging process of 100 A h, 12 V lead acid battery. There are various charging methods used to charge lead-acid batteries such as constant current method, constant voltage method, pulse charge method, float charge method, two stage constant voltage charging etc. The concept adopted in the proposed design is to vary the charging and discharging battery current in order to stabilize the DC link voltage.

The three blocks are used to define the FLC controller are: (i) Fuzzification block, (ii) Inference block and, (iii) Defuzzification block. Fuzzification allows the real variables as fuzzy block inputs and controls the output variable. The DC bus voltage (V_{bus}) is constantly measured. The error $e(k)$ between the DC bus voltage and reference voltage (V_{ref}) and change of error $de(k)$ will be the inputs of fuzzy logic controller at sampling instant k. As shown in Fig. 5a–c, five fuzzy subsets, PB (Positive Big), PS (Positive Small), ZO (Zero), NS (Negative Small) and NB (Negative Big) have been chosen for inputs variables ($e(k)$, $de(k)$) and the output variable (ΔD). Triangular membership functions are used to relate the input and output variables. The range for the input variables $e(k)$ and $de(k)$ is set between [−0.2 0.2] and [–1 1] respectively. The range for output variable (ΔD) is [−1e−5 1e−5]. The fuzzy control rules for error and change of error can be referred in the table shown in Table 1.

$$e(k) = V_{ref} - V_{bus}(k) \tag{8}$$

$$de(k) = e(k) - e(k-1) \tag{9}$$

A rule base is formulated, which can also be expressed in terms of if-then statements. Twenty five fuzzy rules which helps in approximating the output variable were written. In other words, the fuzzy inference block maps the fuzzy input and output variables. The relationship between the input and output variables can also be represented in a (3D) graph as shown in Fig. 5d.

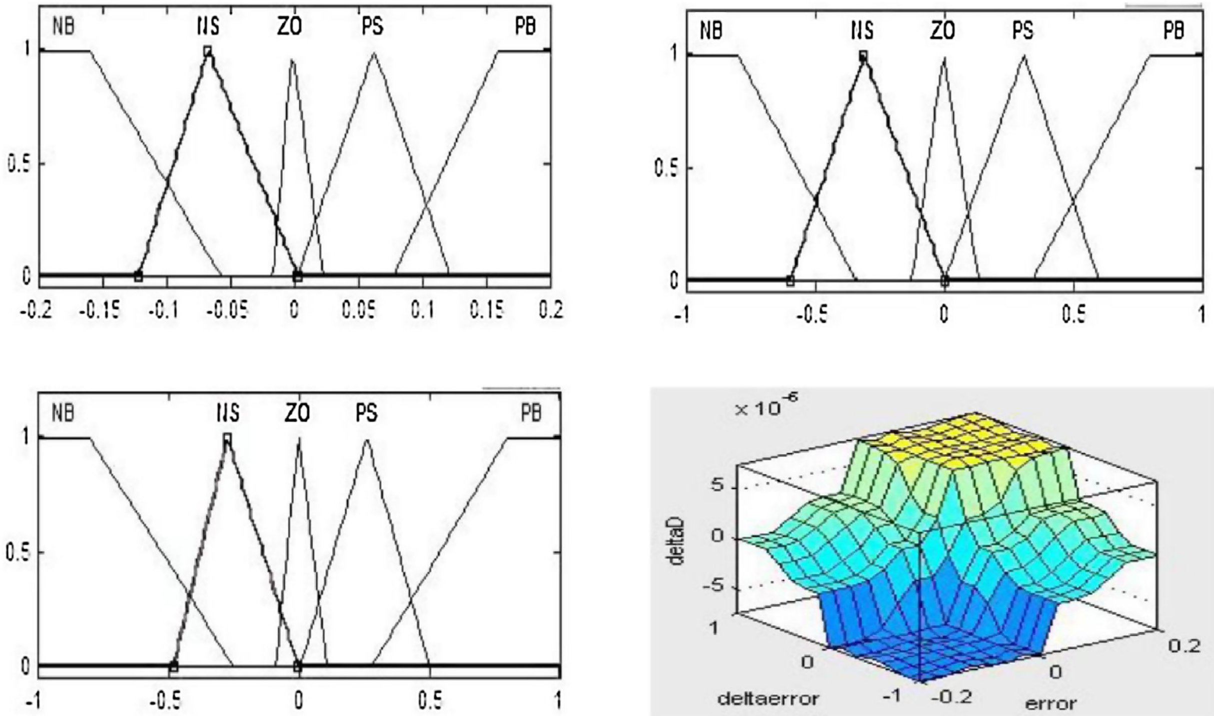

Fig. 5. (a) Distribution of membership functions for input variable (e(k)). (b) Distribution of membership functions for input variable (de(k)). (c) Distribution of membership functions for output variable (4D). (d) 3-D plot for the fuzzy rule base.

Table 1
Rule base for the proposed fuzzy controller.

de(k)	e(k)				
	NB	*NS*	*ZO*	*PS*	*PB*
NB	NB	NB	NB	NS	ZO
NS	NB	NB	NS	ZO	PS
ZO	NB	NS	ZO	PS	PB
PS	NS	ZO	PS	PB	PB
PB	ZO	PS	PB	PB	PB

The main idea behind the rules formulated is to keep the DC link voltage close to the reference voltage either by increasing or decreasing the duty ratio of the bidirectional converter. Therefore, the defuzzification block produces a quantifiable result i.e. the required value of output variable (ΔD) to regulate the bus voltage. The mostly used defuzzification method is Centre of Area (COA) where the output is accomplished by combining the results of the inference process and then computing the fuzzy centroid of the area. The weighted strengths of the output member function is multiplied by the respective output membership function centre points and summed. Finally, this area is divided by the sum of the weighted member function strengths. Mathematically, the output (ΔD) is computed using Eq. (10).

$$\Delta D = \frac{\sum_{j=1}^{n} \mu.\left(\Delta D_j\right).\Delta D_j}{\sum_{j=1}^{n} \mu.\left(\Delta D_j\right)} \tag{10}$$

The fuzzy controller output i.e. the change in duty ratio $\Delta D(k)$, is summed with the recent past value of the duty ratio $D(k\ 1)$. The final output $D(k)$ is computed using Eq. (11).

$$D(k) = D(k-1) + \Delta D(k) \tag{11}$$

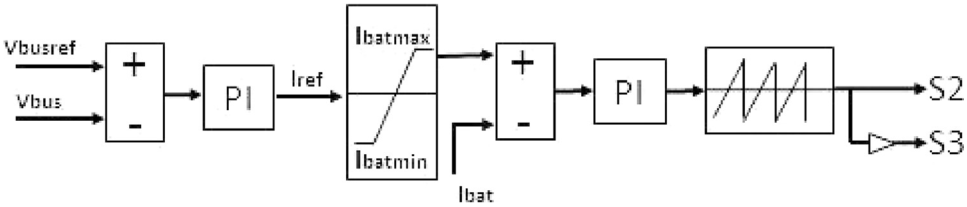

Fig. 6. Cascaded PID controller for bidirectional converter.

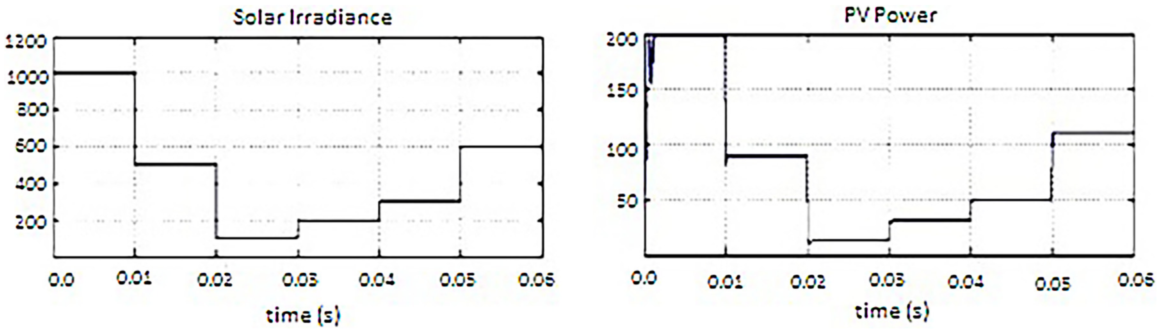

Fig. 7. (a) Variable solar irradiation. (b) Maximum PV power output.

Developing a fuzzy logic controller is simpler and also gives good performance. The design of the controller can be changed depending upon the battery specifications and load requirements.

2.4. PID controller

Fig. 6 depicts the control scheme of the PID controller for bidirectional converter. The bidirectional buck-boost converter is controlled by two cascaded PI controllers comprising of outer voltage control by means of inner current control. DC bus voltage (V_{bus}) is sensed and compared with the DC bus voltage reference (V_{busref}) to produce the error. This error is minimized by the PI controller and current reference (I_{ref}) is produced. This I_{ref} must be limited to maximum allowable charging and discharging currents [I_{batmax}; I_{batmin}] by means of battery current regulation function. The current limits depend on the battery ratings. The current reference is compared with the actual battery current (I_{bat}) and again the error is tuned, producing the complimentary pulses to drive the switches S2 and S3.

3. Simulation results and discussion

Fig. 7b illustrates that PV power output always tracks its maximum value with changing irradiance (G) as shown in Fig. 7a that satisfies the first control objective. The MPPT P&O controller senses the PV module current and voltage to calculate the duty ratio required to drive the boost converter. The design values of the elements used are:(L_1 = 1.33 mH; C_1 = 1 mF; L_2 = 1.5 mH).

As mentioned in Section 2.1, that maximum PV array output power is 200 W at STC condition. It can be verified from Fig. 7b that between t = 0 s to t = 0.01 s, when solar irradiation is 1000 W/m^2, PV output power is matching with its maximum value of 200 W. Similarly, it can be verified for other instants also.

Second objective is fulfilled by current sharing mechanism between battery bank and PV array under variable solar irradiance to achieve a constant DC link voltage. The simulations are carried out to compare the results for FLC and PID controller which are used to regulate power flow from the battery through bidirectional buck-boost converter. The performance of the system such as smoothness of the battery current, battery peak current reduction, settling time and overshoot of the DC link voltage under irradiance change are evaluated. The smoothness of battery current indicates reduced dynamic stress to the battery and reducing the peak current of the battery avoids deep discharging and the battery bank can also be downsized.

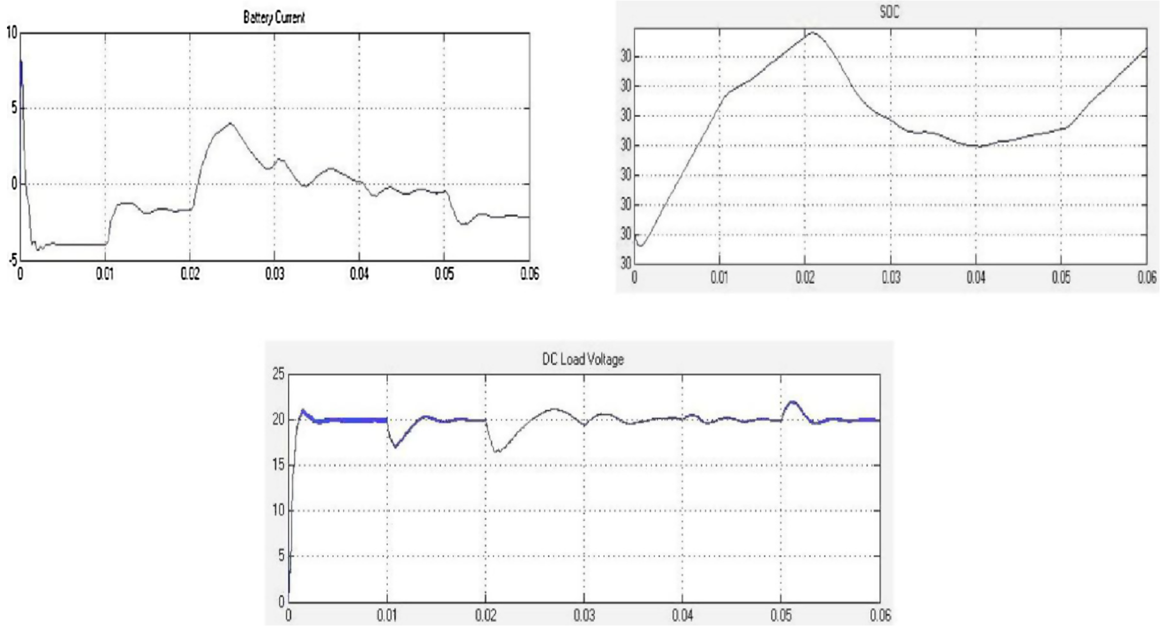

Fig. 8. Results using PID control: (a) Battery current waveform. (b) State of Charge (SOC) of the battery. (c) Regulated DC bus voltage V_{bus}.

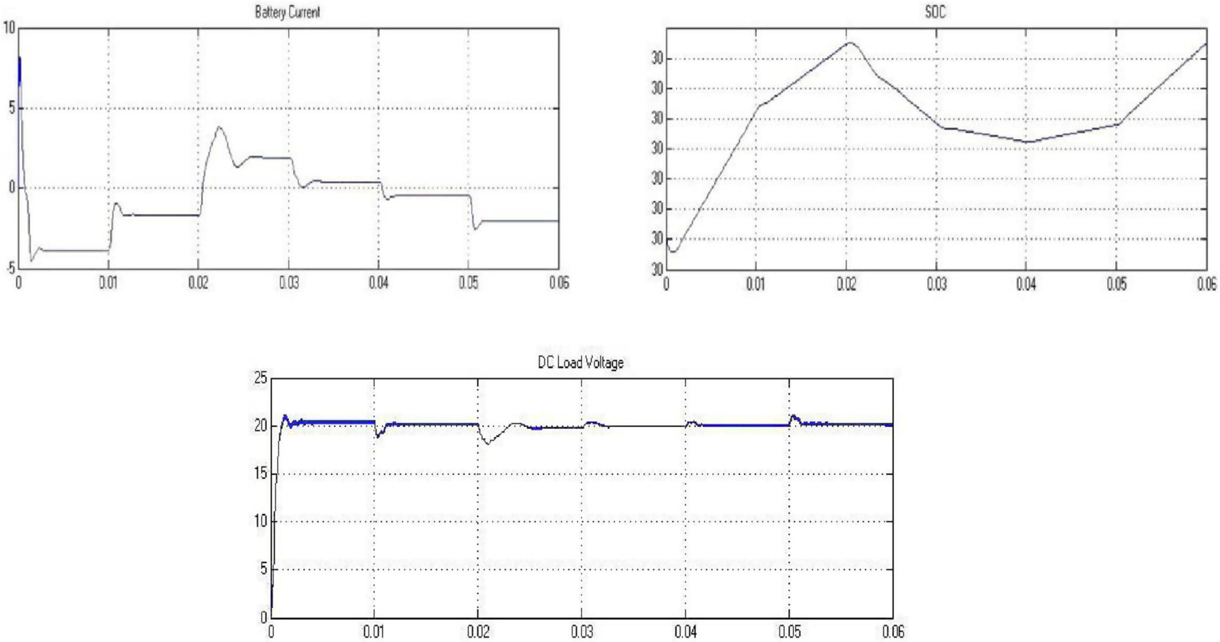

Fig. 9. Results using FLC control: (a) Battery current waveform. (b) State of Charge (SOC) of the battery. (c) Regulated DC bus voltage V_{bus}.

For system with PID controller as shown in Fig. 8(a), the battery always experiences highly fluctuating charging/discharging current. For system with FLC control, Fig. 9(a) shows that the dynamic stress of the battery is slightly improved as compared to the system with PID control. Figs. 9(a) and 8(a) illustrates that the battery peak current is also reduced and besides that, there is improvement in the final SOC of the battery. As shown in fig, the system with FLC control has improved settling time and peak overshoot of the DC link voltage by 16.23% and 14.62% respectively. For the system with FLC control, the strategy reduces the peak current of battery by 0.22%.

4. Conclusion

A Perturb and Observe (P&O) MPPT controller is designed for receiving the maximum power from the PV array under all weather conditions. The resultant system is capable of tracking MPPs accurately and rapidly without steady state oscillations. The comparison of fuzzy controller significantly smoothens the battery current that improves the battery lifespan and also reduces settling time and peak overshoot of the DC link voltage by 16.23% and 14.62% respectively as compared to the system with PID controller.

References

Esram, T., Chapman, P.L., 2007. Comparison of photovoltaic array maximum power point tracking techniques. IEEE Trans. Energy Convers. 22 (2), 439–449.

Faranda, R., Leva, S., 2008. Energy comparison of MPPT techniques for PV systems. WSEAS Trans. Power Syst. 3 (6), 446–455.

Faranda, R., Leva, S., Maugeri, V., 2008. MPPT techniques for PV systems: energetic and cost comparison. Proc. IEEE.

Femia, N., Petrone, G., Spagnuolo, G., Vitelli, M., 2005. Optimization of perturb and observe maximum power point tracking method. IEEE Trans. Aerosp. Electron. Syst. 20 (4), 963–973.

Femia, N., Petrone, G., Spagnuolo, G., Vitelli, M., 2007. Predictive & adaptive MPPT perturb and observe method. IEEE Trans. Aerosp. Electron. Syst. 43 (3).

Garca, P., Torreglosa, J.P., Fernndez, L.M., Jurado, F., 2013. Control strategies for high-power electric vehicles powered by hydrogen FC, battery and SC. Expert Syst. Appl. 40 (September (12)), 4791–4804.

Glavin, M.E., Chan, P.K.W., Armstrong, S., Hurley, W.G., 2008. A standalone photovoltaic supercapacitor battery hybrid energy storage system. In: Proc. 13th Power Electron. Motion Control Conf., September 1–3, pp. 1688–1695.

Guiting, X., Yan, Z., Dakang, Z., 2013. Synthetically control of a hybrid PV/FC/SC power system for standalone applications. J. Appl. Sci. 5 (5), 1796–1803.

Rohrig, Kurt, Lange, Bernhard, 2008. Power and Energy Society General Meeting — Conversion and Delivery of Electrical Energy in the 21st Century, 1–6.

Salas, V., Olias, E., Barrado, A., Lazaro, A., 2006. Review of the maximum power point tracking algorithms for stand-alone photovoltaic systems. Sol. Energy Mater. Sol. Cells 90 (11), 1555–1578.

Thounthong, P., Rael, S., Davat, B., 2009. Energy management of FC/Battery/SC hybrid power source for vehicle application. J. Power Sources 190 (May (1)), 173183.

Thounthong, P., Luksanasakul, A., Koseeyaporn, P., Davat, B., 2013. Intelligent model-based control of a standalone photovoltaic/fuel cell power plant with supercapacitor energy storage. IEEE Trans. Sustain. Energy 4 (January (1)), 240–249.

Torreglosa, J., Garcia, P., Fernandez, L., Jurado, F., 2014. Predictive control for the energy management of a FC battery SC tramway. IEEE Trans. Ind. Inform. 10 (February (1)), 276285.

Weddell, A.S., Merrett, G.V., Kazmierski, T.J., Al-Hashimi, B.M., 2011. Accurate supercapacitor modeling for energy harvesting wireless sensor nodes. IEEE Trans. Circuits Syst. II: Exp. Brief 58 (December (12)), 911915.

Zegaoui, A., Aillerie, M., Petit, P., Sawicki, J.P., Jaafar, A., Salame, C., Charles, J.P., 2011. Comparison of two common maximum power point trackers by simulating of PV generators. Energy Procedia 6, 678–687.